RSC Advances

ROYAL SOCIETY OF CHEMISTRY

www.rsc.org/advances

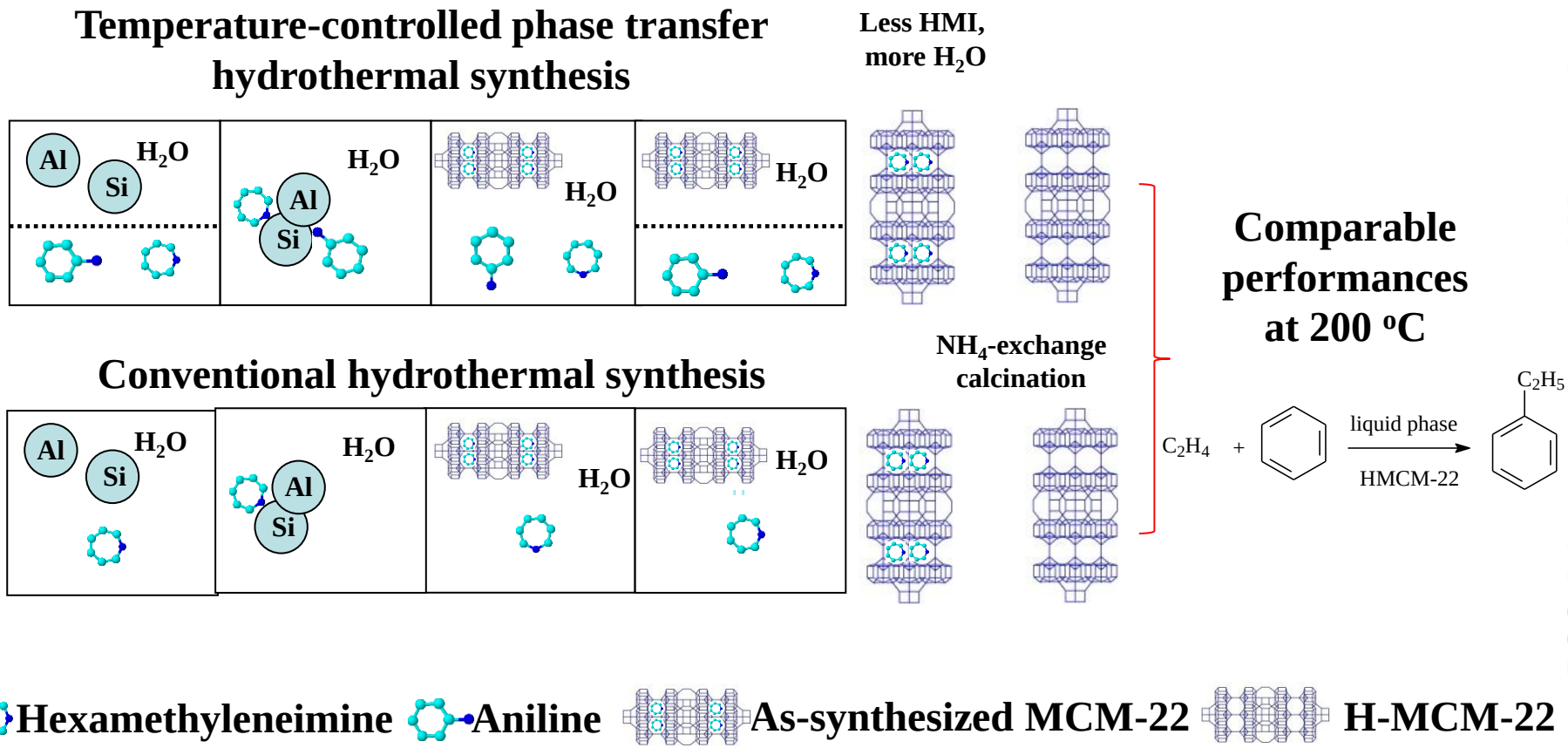

Synthesis, characterization and application of MCM-22 zeolites synthesized via conventional HMI route and temperature-controlled phase transfer hydrothermal synthesis

Enhui Xing, Yanchun Shi, Wenhua Xie, Fengmei Zhang*, Xuhong Mu and Xingtian Shu

State Key Laboratory of Catalytic Materials and Reaction Engineering, Research Institute of Petroleum Processing, Sinopec, Beijing 100083, China

*Corresponding author: Prof. Fengmei Zhang

Address: Research Institute of Petroleum Processing Sinopec, Xueyuan Road 18, Beijing, China.

Tel: +86 010-82368698

E-mail: zhangfm.ripp@sinopec.com (F. M. Zhang)

Abstract:

With less environmental and economical impacts, temperature-controlled phase transfer hydrothermal synthesis of MWW zeolites was realized with hexamethyleneimine as a structure-directing agent and aniline as a structure-promoting agent. MCM-22 zeolite, synthesized via temperature-controlled phase transfer hydrothermal synthesis, is nearly identical concerning chemical composition and structure, and possesses nearly identical properties with respect to porosity, Si/Al ratio, thermal behavior and catalytic activity at 200 °C, compared with that made from conventional synthesis with hexamethyleneimine as the only template.

Keywords: **MCM-22; Temperature-controlled phase transfer hydrothermal synthesis; Liquid-phase alkylation; ethylbenzene**

1. Introduction

MCM-22 zeolite (IZA code MWW), firstly synthesized by Mobil researchers, represents an original zeolite with the combination of two classes of materials: zeolites and layered solids, which presents two independent pore systems: two-dimensional, sinusoidal, 10 MR intralayer channels and 12MR interlayer supercages, both accessible through 10 MR apertures.[1, 2] There is a family of materials with a structure related to MWW, such as MCM-22, MCM-49, and MCM-56, where the differences between them are mainly due to the packing degree of the layers; MCM-49 (Ref. 3) possesses the identical framework topology as calcined MCM-22, and MCM-56 (Ref. 4) maintains the single-layered structure on calcination. Related materials are the aluminosilicate SSZ-25 (Ref. 5), the boron-containing analog ERB-1 (Ref. 6), and the pure silica polymorph ITQ-1 (Ref. 7). MWW zeolites are usually synthesized by the utilization of cyclic amines and organic cations as templates. For aluminosilicates MWW zeolites (MCM-22, MCM-49, MCM-56 and SSZ-25), hexamethyleneimine (HMI) is one of the most usually used templates. Severe toxicity and difficulty in recovery of HMI are the major challenges for the hydrothermal synthesis of MWW zeolites.[8-10]

Previously we reported a novel hydrothermal synthesis concept of MCM-22 and MCM-49 zeolites entitled as "Temperature-controlled phase transfer hydrothermal synthesis" with HMI as a structure-directing agent (SDA) and aniline (AN) as a structure-promoting agent.[8] There are several features of the temperature-controlled phase transfer hydrothermal synthesis. (1) Aniline is insoluble in mother liquid and HMI is extracted to aniline phase at room temperature. (2) At crystallization temperature, the aniline and HMI become completely soluble in mother liquid to promote crystallization. (3) After crystallization, with the decrease of temperature, aniline becomes insoluble

again to achieve an automatic integrated process of phase separation and extraction of unincorporated HMI from as-synthesized MWW zeolites and mother liquid to organic phase. The involvement of aniline has three unexpected functions: (1) Aniline acts as a structure-promoting agent to fill pores of MWW zeolites during crystallization. Little incorporated aniline is detected on as-synthesized MWW zeolites; (2) Aniline is the phase transfer medium to achieve temperature-controlled phase transfer hydrothermal synthesis; (3) Aniline is the extractor to extract HMI to organic phase for the recovery of HMI and aniline. On the whole, aniline is more like a "catalyst" of the "temperature-controlled phase transfer hydrothermal synthesis" of MWW zeolites. On one hand, the involvement of aniline as a structure-promoting agent significantly decreases the needed amount of HMI as the SDA by 2/3. On the other, it makes the complete recycle and reuse of HMI and aniline achievable with additional distillation process. Even without additional distillation process, most of HMI and aniline can be recycled and reused with a simple liquid separation.

This paper reports the sequential results of "temperature-controlled phase transfer hydrothermal synthesis". Detailed characterizations of MCM-22 zeolites were performed to reveal the differences between conventional HMI samples and HMI/AN samples. Also the liquid-phase alkylation of benzene with ethylene over MCM-22 catalysts (HMI and HMI/AN) was performed to find whether the involvement of aniline as a structure-promoting agent and the decrease of HMI usage would influence catalytic performances of MCM-22 catalysts.

2. Experimental

2.1 Synthesis of MWW zeolites

Samples of MCM-22 and MCM-49 were produced in accordance with procedures outlined elsewhere.[1, 3 and 8] All materials (silica gel, $NaAlO_2$, NaOH, HMI, aniline and deionized water) were used as purchased. The typical batch composition in terms of molar ratio was: SiO_2/Al_2O_3 = 20 ~ 30, $NaOH/SiO_2$ = 0.18, R/SiO_2 = 0.30, H_2O/SiO_2 = 15, if without specific description. The hydrothermal synthesis was carried out for 72 h in a Teflon-lined autoclave under rotating condition (30 r/min) at 145 °C. The products were filtered, washed with water until pH value = 7, and dried at 100 °C overnight. The as-made material synthesized in the presence of only HMI was named MCM-22P (HMI). The as-made material synthesized in the presence of HMI and aniline was named MCM-22P (HMI/AN). All samples were calcined at 550 °C in ambient air for 6 h in a muffle furnace to remove organics. The calcined materials free of organic materials obtained from the precursor MCM-22P (HMI) and MCM-22P (HMI/AN) were named MCM-22C (HMI) and MCM-22C (HMI/AN), respectively.

2.2 Characterization of MWW zeolites

X-ray diffraction (XRD) patterns of samples were collected on a D/MAX-III X-ray diffractometer (Rigaku Corporation, Japan) with filtered Cu K α radiation at a tube current of 35 mA and a voltage of 35 kV. The scanning range of 2 θ was 5 ~ 35 °. The crystal morphology was measured on a FEI Quanta scanning electron microscope (SEM). The elemental analyses of the solids were performed on an X-ray fluorescence (XRF) spectrometer MagiX (Philips). Nitrogen adsorption-desorption isotherms were recorded on a Micromeritics ASAP 2010 instrument. The samples were first outgassed under vacuum at 363 K for 1 h and at 623 K for 15 h. The total surface area was obtained by application of the BET equation using the relative pressure range of 0.05 - 0.16 in the nitrogen adsorption isotherm as range of linearity (using a molecular

cross-sectional area for N_2 of 0.162 nm^2). The micropore volume was calculated by the t-plot method.

^{29}Si MAS NMR experiments were performed on a Bruker AVANCE III 500WB spectrometer at a resonance frequency of 99.3 MHz using a 7 mm double–resonance MAS probe with a recycle delay of 4 s. The magic-angle spinning speed was 5 kHz in all experiments, and a typical $\pi/6$ pulse length of 1.8 μs was adopted for ^{29}Si resonance. The chemical shift of ^{29}Si was referenced to tetramethylsilane (TMS).

^{27}Al MAS NMR experiments were performed on a Bruker AVANCE III 600WB spectrometer at a resonance frequency of 156.4 using a 4 mm double-resonance MAS probe at a sample spinning rate of 13 kHz. The chemical shift of ^{27}Al was referenced to 1 M aqueous Al $(NO_3)_3$. ^{27}Al MAS NMR spectra were recorded by small-flip angle technique using a pulse length of 0.4 μs ($<\pi/15$) and a recycle delay of 1 s.

TG-MS was performed on the NETZSCH STA409PC (TG)-QMS403C (MS). TG profiles were collected out with conditions as following: carrier: air, 50 °C to 600 °C, 10 °C /min. The ionization source of MS that coupled with TG was electron impact (EI) with an ionization voltage of 70 eV. The bargraph cycles of mass-to-charge ratio (m/z) were from 1 to 300. The sensitivity was 100 ppb with a standard single filter quadrupole mass analyzer. Gas concentrations were tracked at a sampling rate of 1 data points/min for a simple data analysis.

2.3 Preparation of H-MCM-22 catalysts

The MCM-22P samples were ion-exchanged twice in NH_4NO_3 solution at 90 °C for 2 h, to obtain the corresponding NH_4-type samples with Na_2O content less than 0.05 wt.%. The composition among MCM-22P zeolites, NH_4NO_3, and deionized water on the basis of mass ratio was: 1:1:20. The NH_4-type samples (70 wt. %) and Al_2O_3 (30

wt. %) were mixed and extruded. The Al_2O_3, which show almost no activity in liquid-phase alkylation of benzene with ethylene, was used as binder to increase the mechanical strength of catalysts. The extruded catalysts were then scrapped to collect the granules with a griddle of 16 ~ 20 mesh and then subjected to calcinations at 550 °C for 6 h to obtain corresponding H-type catalysts. The H-type catalysts derived from MCM-22 (HMI) and MCM-22 (HMI/AN) were named as H-MCM-22 (HMI) and H-MCM-22 (HMI/AN) catalysts.

2.4 Liquid-phase alkylation of benzene with ethylene

The liquid-phase alkylation of benzene with ethylene over H-MCM-22 catalysts was performed in a ten-staged reactor in series. In a typical catalyst evaluation, 8 mL of catalyst was loaded on the middle of the each stainless reactor. The reactor was then brought to the reaction temperature of 200 ^oC where the alkylation was operated continuously at 3.5 MPa, the individual/total benzene to ethylene molar ratio of 20.0/2.0 and weight hourly space velocity (WHSV) of 1.5 h^{-1} for ethylene, 200 ^oC to 260 ^oC of temperature. The reaction products were not collected until every temperature point lasted for at least 15 h, by three times a day, which ensured that the reaction was completely stable. The reaction products were analyzed by an Agilent 6890 gas chromatograph (GC) equipped with a flame ionization detector and a capillary column.

3 Results and discussion

3.1 The synthesis of MWW zeolites

The hydrothermal synthesis results of MWW zeolites with different SiO_2/Al_2O_3 ratios are shown in Table 1. All products showed relative lower SiO_2/Al_2O_3 ratios than the corresponding feeding gel SiO_2/Al_2O_3 ratios in alkaline solution. With feeding gel

SiO_2/Al_2O_3 ratios at 30, MCM-22 was obtained in both HMI and HMI/AN systems. While with feeding gel SiO_2/Al_2O_3 ratios at 20, the MCM-49 was formed. It has been proved that feeding gel SiO_2/Al_2O_3 ratio was one of the key factors to the formation of MCM-22 and MCM-49. Higher feeding gel SiO_2/Al_2O_3 ratio favored the formation of MCM-22; while the lower feeding gel SiO_2/Al_2O_3 ratio led to the formation of MCM-49 (Ref. 3). It is very interesting that, for samples with feeding gel SiO_2/Al_2O_3 ratios at 25, MCM-22 was yielded in the HMI system, while MCM-22/49(more) in the HMI/AN system. As well known, H-bonded HMI accounted for the formation of MWW layers. For the HMI/AN system, less usage of HMI meant less HMI to sustain single MWW layer to avoid the formation of oxygen bridging between Si-OH because of the failure of aniline as the template, [8] which was in accordance with the Mobil's results that the formation of MCM-49 was favored with HMI/Na^+ less than 2.0 (Ref. 3). For samples with feeding gel SiO_2/Al_2O_3 ratios at 25 the involvement of aniline led to lower HMI/Na^+ to strengthen the tendency of MCM-49 formation. In all, MCM-49 is much easier to be generated in HMI/AN system than in the HMI system.

As shown in Fig. 1, MCM-22P showed the typical (002) diffraction peak at ca. 6.6° 2 theta due to the layer stacking of the MWW sheets. After calcination at 550 °C in a muffle furnace for 6 h, the organic species were completely removed. Meanwhile, interlayer dehydroxylation and condensation took place to generate 3D MWW structure. The XRD patterns of the calcined samples showed well-resolved characteristic peaks of 3D MWW topology in the range of 2 theta = 5 ~ 35 ° without other crystalline phases and amorphous phase. This confirmed the formation of MCM-22C and MCM-49 with high crystallinity. Another region that distinguishes MCM-22P from MCM-49 and MCM-22C occurs between 26 and 29 °, illustrated in Fig. 1. In MCM-22P only one

peak occurs in this region and is centered at 26.22 °. It is broad and has a smooth, sloping tail that is visible on the high 2 theta side. For MCM-49 and MCM-22C this feature is replaced by three sharp peaks, occurring in the approximate region 26.5 ~ 29.0°. In all, there were no obvious differences in the synthesis of MWW zeolites except that the involvement of aniline increases the tendency to MCM-49 formation in the HMI/AN system, in which lower HMI/Na^+ is achieved by the involvement of aniline.

3.2 Texture properties and crystal morphology of MCM-22 zeolites

The compositions, surface areas and pore volumes of MCM-22C (HMI) and MCM-22C (HMI/AN) are shown in Table 2, which indicates that the compositions and most of textural properties of MCM-22C (HMI) and MCM-22C (HMI/AN) are similar except total pore volumes. The BET surfaces and micro pore surfaces of MCM-22C (HMI/AN) are 462 $m^2 \cdot g^{-1}$ and 382 $m^2 \cdot g^{-1}$ respectively, which are almost same as those of MCM-22C (HMI) regardless of slight difference. Although the total volume of the MCM-22C (HMI/AN) is 0.534 $cm^3 \cdot g^{-1}$, lower by about 10% than that of the MCM-22C (HMI), the micro pore volume of MCM-22C (HMI/AN) is 0.178 $cm^3 \cdot g^{-1}$, slightly higher than that of the MCM-22C (HMI). Although the two samples are severely accumulated, both of them have clear layer assembled rose like shape with diameter at about μm level (Fig. 2), which is usually encountered in the synthesis with solid silica gel as raw material. In all, it seemed that the involvement of aniline as a structure-promoting agent had no obvious effects on the properties of MCM-22 zeolites compared to the conventional MCM-22 with HMI as the only structure-directing agent.

3.3 The NMR characterization of MCM-22 zeolites

As shown in Fig. 3, the ^{29}Si MAS NMR spectra of the as-synthesized samples are

similar to those presented in previous literature, [11-19] with five peaks at about -119, -115, -113, -110 and -100 ppm. These peaks were mainly associated with Si sites of MWW zeolites as following: -100 ppm ~ Si (1Al) and -105 ppm to -119 ppm ~ Si (0Al). Both of HMI and HMI/AN samples showed similar ^{29}Si MAS NMR spectra, so did calcined samples. Therefore, the involvement of aniline into the synthesis did not lead to obvious changes of framework Si.

The ^{27}Al MAS NMR spectra of framework aluminosilicates usually consist of one or more tetrahedral Al resonances in the 45-65 ppm region of the spectrum that reflects the average environment of Al atoms in the tetrahedral framework (Fig. 4). The ^{27}Al MAS NMR spectra of MCM-22P were both comprised of at least two tetrahedral Al resonances centered at ~50 and~56 ppm.[11-19] Upon calcination, the shoulder at 49 ppm was further reduced while the resonance at about 60 ppm also appeared as a shoulder and was more visible. Lawton[3] reported similar spectra, with the resonance at 49 ppm clearer at higher fields. As for calcined samples, both HMI and HMI/AN samples showed the occurrence of extra-framework aluminum, caused by high temperature calcinations. A sharp peak at about 0 ppm due to octahedral aluminum can be clearly observed, indicating that calcinations cause dealumination to some extent. This peak was also present for the calcined samples of Lawton, [3] however Ravishankar[13] and Hunger[16] reported this peak to be much smaller than ours. It should be noticed that the latter two groups used milder conditions during calcination (lower temperatures and/or reduced oxygen concentration). No significant differences were observed between the spectra of our samples (HMI and HMI/AN) and those of samples prepared by other authors.

For framework components, the environments of Si and Al showed no obvious

changes due to the involvement of aniline into the synthesis. The only observable change was that the ^{13}C CP MAS NMR of HMI at 57 ppm was dramatically diminished with resonances at 49 ppm slightly decreased, which was caused by aniline as reported in our previous communication.[8]

3.4 TG-MS characterization of MCM-22P zeolites

As revealed in our previous paper, usually MCM-22C (HMI/AN) shows higher relative crystallinity as MCM-22C (HMI) with other conditions unchanged. It is deduced that lower HMI content of MCM-22P (HMI/AN) leads to fewer loss of relative crystallinity during calcinations. In order to testify above deduction, TG-MS was used to investigate the oxidative decomposition of HMI incorporated in as-synthesized zeolites.

Generally speaking, for MWW zeolites, the Na_2O/Al_2O_3 ratio is much lower than one for all crystalline materials, which indicates that the negative charge of the framework due to Al content is compensated by protonated HMI. The amount of organic material is higher than the aluminum determined by chemical analysis. It should correspond to protonated amine-neutralizing framework Al and organic species occluded into the cavities.[14] Mobil researchers concluded[3] that HMI resided in two distinct environments and led to a difference in the pathway by which HMI is desorbed. Low-temperature desorption peak was associated with HMI in the interlayer region, while high-temperature desorption peak was associated with HMI in the intralayer channel, which could only be removed by high temperature decomposition. TG-MS tests in air were conducted to testify the oxidative decomposition behaviors of organics incorporated into as-synthesized samples via conventional and HMI/AN induced temperature-controlled phase transfer hydrothermal synthesis.

Fig. 5 shows the TG curves of as-synthesized samples. It is very interesting that MCM-22P (HMI) and MCM-22P (HMI/AN) had almost the same weight losses until 600 °C, while they showed different TG curves. Obviously, there were four kinds of desorption temperature-dependent weight losses: zone 1 with temperature < 100 °C , zone 2 with temperature from 100 °C to 200 °C, zone 3 from temperature 200 °C to 350 °C and zone 4 with temperature above 350 °C. Below 100 °C, the MCM-22P (HMI) gives slower and smaller weight loss than the MCM-22P (HMI/AN). Between 100 °C to 200 °C, both of the two samples show slight weight losses. From 200 °C to 350 °C, the MCM-22P (HMI) shows faster weight loss than the MCM-22P (HMI/AN). Above 350 °C, both of two samples show almost the same curves of oxidative desorption even with the same starting and final ending points, which indicated that the amount and the behaviors of HMI incorporated in as-synthesized samples at higher temperature (> 350 °C) were almost same. The desorption at higher temperature (> 350 °C) was surely associated with the protonated HMI to compensate the negative charge of Al, which needed more energy to decompose or desorb from as-synthesized samples. Similarity of desorption curves in shape meant that there was only one kind of protonated HMI incorporated in as-synthesized samples. The almost same weight losses at higher temperature indicated that same SiO_2/Al_2O_3 of the gel and the products meant the same content of Al, which should be balanced by the same amount of protonated HMI. As proved in our previous paper, aniline was not detected with sufficient intensities by ^{13}C CP MAS NMR, which could exclude the possibility of aniline incorporated in the as-synthesized samples. Compared with the MCM-22P (HMI), lower HMI usage in the HMI/AN system did not lead to the less weight loss of the MCM-22P (HMI/AN), but changed the desorption behavior of the as-synthesized sample, that is, aniline did

influence the hydrothermal synthesis and the zeolites in spite of no detection of aniline in as-synthesized sample. What interests us most is what compensated the weight loss of the MCM-22P (HMI/AN), or why aniline makes HMI easier to be incorporated in as-synthesized sample at lower HMI/SiO_2 ratio? The major concerns are focused on the zone 1 and zone 3 with the obviously different desorption curves. In order to verify these, TG-MS was used to monitor the decomposition products of the as-synthesized samples.

Altogether, there were 17 peaks detected with sufficient MS signal intensities, whose m/z were at 16, 17, 18, 27, 28, 30, 39, 41, 42, 43, 44, 46, 48, 55, 56, 57 and 64 respectively. The peak with m/z = 16 (Fig. 6) was associated with -NH_2 rather than O and CH_4, because no detection of the peaks with m/z = 32 for O_2 and m/z = 15 for CH_3 fragment. The decomposed -NH_2 was surely originated from HMI molecules rather than protonated HMI, because desorption of protonated HMI only occurred at higher temperature above 350 °C. Generally, the –NH_2 could be associated with NH_3 or HMI. In the case of samples tested in this paper, the –NH_2 originated from HMI rather than NH_3. The reasons lied in the completely different curves with m/z = 16 and 17. The decomposition of HMI incorporated in as-synthesized samples in the atmosphere of N_2 or He had seldom been referred to proceed in temperature below its boiling point. As for the curve with m/z = 18 (Fig. 6) was obviously originated from H_2O. The desorption at lower temperature was associated with physical adsorbed water molecules, while dehydration of zeolite two surface hydroxyl groups began to lose one water molecule to from oxygen bridging, which resulted in the desorption peak of water at temperature >350 °C. The curve with m/z = 17 was associated with HO rather than NH_3 because of its similarity to the desorption curve with m/z = 18. The weight loss below

350 °C was mainly due to -NH_2, -HO and H_2O. Obviously with the combination of TG curves, the MCM-22P (HMI) had higher HMI content to afford more -NH_2 by approximate 33%, while the MCM-22P (HMI/AN) had more water to desorb, which accounted for the fast weight loss below 100 °C. Considering our previous hypothesis that HMI/AN sample had more water molecules to stabilize framework because of the drive of aniline out of zeolite framework by phase separation induced by temperature, TG-MS curves proved the higher content of water molecules incorporated in the MCM-22P (HMI/AN), which could be dehydrated at temperature lower than 100 °C. Desorption of water molecules incorporated in MWW zeolite surely led to fewer loss of relative crystallinity caused by decomposition of HMI.

As shown in Fig. 7 and 8, incomplete oxidation led to the formation of CO (m/z = 28) and NO (m/z = 30). With the increase of the temperature, complete oxidation products such as CO_2 (m/z = 44) and NO_2 (m/z = 44) occurred, which only happened at temperature higher than 350 °C. In general, the pollutants of calcination of MWW samples were NO and CO at lower temperature, CO_2 and NO_2 at higher temperature.

Curves of C2, C4 and C3 fragments with m/z = 27, 55, 56, 57, 41, 42 and 43 (Fig. S1 to S7) occurred at higher temperature (above 350 °C), which were the oxidative decomposition products of protonated HMI. In such a way, protonated HMI decomposed into C2/C4 and C3 fragment ions. With air as carrier, the oxidative decomposition proceeded so easily and suddenly that the decomposition products could be neglected with the comparison with oxidative products such as CO and CO_2.

In general, the MCM-22P (HMI) and MCM-22P (HMI/AN) samples show similar decomposition curves with the differences in peak intensities, which reveals that only HMI is incorporated in the as-synthesized the MCM-22P (HMI/AN). If there was

aniline incorporated in the MCM-22P (HMI/AN), there surely should have different decomposition curves, what's more, no detection of C_6H_6 or C_6H_5 fragments also excluded the incorporation of aniline into as-synthesized HMI/AN sample. This results support our previous conclusion that aniline acts as a structure-promoting agent to fill pores of MWW zeolites during crystallization and that after crystallization with the decrease of temperature the aniline is driven out of the as-synthesized samples. From the view of catalysis, the aniline, the structure-promoting agent, acts as the "catalyst" to promote the hydrothermal synthesis of MWW zeolites without any consumption of itself. Little incorporated aniline is detected on the as-made zeolites.

3.5 Catalytic properties of H-MCM-22 in liquid-phase alkylation of benzene with ethylene

The catalytic activities and product distributions were compared between H-MCM-22 (HMI) and H-MCM-22 (HMI/AN) catalysts with the same feeding gel SiO_2/Al_2O_3 ratios at 30. The alkylation of benzene with ethylene was operated in the ten-staged reactors in series under liquid-phase at 3.5 MPa from 200 °C to 260 °C. The reaction products were made up of ethylbenzene (EB), xylenes (Xys), para-diethylbenzene (p-DEB), ortho-diethylbenzene (o-DEB), meta-diethylbenzene (m-DEB), triethylbenzenes (TEB), C9–C11 and other by-products.[20-24] These two catalysts have very comparable bulk SiO_2/Al_2O_3 ratios and textual properties. The ethylene conversion and ethylbenzene selectivity of HMI and HMI/AN catalysts were listed in Table 3. The ethylene conversion of both H-MCM-22 (HMI) and H-MCM-22 (HMI/AN) catalysts increased with the increase of reaction temperature, while the EB selectivity changed in a reverse direction. The dependency of the ethylene conversion and EB selectivity on reaction temperature was reported everywhere. Generally

speaking, the reaction temperature is one of the key factors to influence the ethylene conversion and EB selectivity. Usually, the reaction temperature was selected at the range where alkylation of benzene with ethylene is high. As shown in Table 3, the H-MCM-22 (HMI) catalyst yielded the lower ethylene conversion, but better EB selectivity with temperature higher than 200 °C. The H-MCM-22 (HMI/AN) catalyst showed higher ethylene conversion, but poorer EB selectivity. Obviously the suitable reaction temperature should be 200 °C, at which the H-MCM-22 (HMI/AN) catalyst showed almost the same ethylene conversion and EB selectivity as the H-MCM-22 (HMI) catalyst. Also, as shown by Table 4, there seemed little difference in the distribution of DEBs and TEBs at 200 °C. Based upon our previous results, MWW zeolites could be manufactured in a much cheaper and greener way by the utilization of aniline as a structure-promoting agent, which led to the discovery of temperature-controlled phase transfer hydrothermal synthesis to achieve easy and complete recovery of HMI with severe toxicity.

Although there are several synthetic strategies to MWW zeolites, such as HMI/ cyclohexylamine, piperdine and quaternary ammonium hydroxides, almost few results about their catalytic properties are reported. Most of alkylation of benzene with ethylene was conducted over MWW zeolites directed by HMI only. Maybe this is the first report of the H-MCM-22 (HMI/AN) catalyst about their catalytic properties. However the involvement of aniline leads to the greener and cheaper method of producing MWW zeolites without any obvious influences on its catalytic performance.

4. Conclusion

MWW zeolites were synthesized by conventional synthesis with HMI as the only SDA and temperature-controlled phase transfer hydrothermal synthesis with HMI as a

structure-directing agent and aniline as a structure-promoting agent. About 2/3 decrease in the amount of HMI leads to no obvious differences in the properties of MCM-22 zeolite with aniline as a structure-promoting agent, which is a more economical and greener route for MWW zeolites' synthesis. The major difference lies in that HMI/AN favors the formation of MCM-49, due to lack of sufficient HMI to protect Si-OH through hydrogen bond to avoid the formation of oxygen bridging, which is the key step to the formation of MCM-49. Similarity in oxidative curves also supports the conclusion that there is almost no aniline incorporated in the as-synthesized samples, that is, only HMI is incorporated. At 200 °C, the H-MCM-22 (HMI/AN) catalyst shows almost the same ethylene conversion and ethylbenzene selectivity as the H-MCM-22 (HMI) catalyst, however MWW zeolites could be manufactured in a much cheaper and greener way by the utilization of aniline as a structure-promoting agent, which leads to the discovery of temperature-controlled phase transfer hydrothermal synthesis to achieve easy and complete recovery of HMI of severe toxicity.

Previous investigations of HMI/AN induced temperature-controlled phase transfer hydrothermal synthesis were mainly focused on reducing the amount of severely toxic HMI with other considerations neglected. As proved in our previous paper, there is no aniline consumption during the whole process of temperature-controlled phase transfer hydrothermal synthesis of MWW zeolites, in which aniline as "catalyst" are not incorporated, could be recovered and reused in the following synthesis. Aniline and unincorporated HMI could be recycled and reused with the help of the following supplementary units for liquid phase separation and distillation. Even with more HMI and aniline involvements, the separation, recovery and the reuse of the organic phase could be easily achieved with no more modification of units, but larger recovered water.

In all, future works will surely focus on the influence of HMI/SiO_2 and AN/SiO_2 ratios, which may be the crucial factor to adjust the textual and acidic properties of the MWW zeolites.

Acknowledgments

This work was supported by the National Basic Research Program of China (973 Program, No.2012CB224805). Special thanks to the Department of Analysis in Research Institute of Petroleum Processing Sinopec.

References

1. M. K. Rubin and P. Chu, US patent 4,954,325, 1990.
2. M. E. Leonowicz, J. A. Lawton, S. L. Lawton and M. K. Rubin, *Science*. 1994, **264,** 1910-1913.
3. S. L. Lawton, A. S. Fung, G. J. Kennedy, L. B. Alemany, C. D. Chang, G. H. Hatzikos, D. N. Lissy, M. K. Rubin, H. C. Timken, S. Steuernagel and D. E. Woessner, *J. Phys. Chem.,* 1996, **100,** 3788-3798.
4. W. J. Roth, *Stud. Surf. Sci. Catal.,* 2005, **158,** 19-26.
5. S. I. Zones, S. J. Hwang and M. E. Davis, *Chem. Eur. J.,* 2001, **7,** 1990-2001.
6. R. Millini, G. Perego, W. O. Parker Jr, G Bellussi and L. Carluccio, *Microporous Mater.,* 1995, **4,** 221-230.
7. M. A. Camblor, A. Corma, M. J. Díaz-Cabañas and C. Baerlocher, *J. Phys. Chem. B.*, 1998, **102,** 44-51.
8. E. H. Xing, X. Z. Gao, W. H. Xie, F. M. Zhang, X. H. Mu and X. T. Shu, *RSC adv.,* 2014, **4,** 24893-24899.
9. W. H. Lai and R. E. Kay, US patent 7,799,316. 2010.

10. W. H. Lai and R. E. Kay, US patent 8,080,234. 2011.
11. A. L. S. Marques, J. L. F. Monteiro and H. O. Pastore, *Micropor. Mesopor. Mater.,* 1999, **32,** 131-145.
12. D. Vuono, L. Pasqua, F. Testa, R. Aiello, A. Fonseca, T.I. Koranyi and J.B. Nagy. *Micropor. Mesopor. Mater.,* 2006, **97,** 78-87.
13. R. Ravishankar, T. Sen, V. Ramaswamy, H. S. Soni, S Ganapathy and S. Sivasanker, *Stud. Surf. Sci. Catal.,* 1994, **84,** 331-338.
14. A. Corma, C. Corell and J. Pérez-pariente, *Zeolite,* 1995, **15,** 2-8.
15. W. Kolodziejski, C. Zicovich-Wilson, C. Corell, J. Pérez-pariente and A. Corma, *J. Phys. Chem.,* 1995, **99,** 7002-7008.
16. M. Hunger, S. Ernst and J. Weitkamp, *Zeolite,* 1995, **15,** 188-192.
17. G. J. Kennedy, S. L. Lawton and M. K. Rubin, *J. Am. Chem. Soc.,* 1994, **116**, 11000-11003.
18. G. J. Kennedy and S. L. Lawton, *Microporous M*ater., 1997, 9, 209-212.
19. M. J. Cheng, D. L. Tan, X. M. Liu, X. W. Han, X. H. Bao and L. W. Lin, *Micropor. Mesopor. Mater.,* 2001, **42,** 307-316.
20. J. C. Cheng, C. M. Smith, C. R. Venkat and D. E. Walsh. US patent 5,600,048, 1997.
21. J. Cheng, T. Degnan, J. Beck, Y. Huang, M. Kalyanaraman, J. Kowalski, C. Loehr and D. Mazzone, *Stud. Surf. Sci. Catal.,* 1999, **121**, 53-60.
22. K. F. Liu, S. J. Xie, G. L. Xu, Y. N. Li, S. L. Liu and L. Y. Xu. *Appl. Catal. A: Gen.,* 2010, **383,** 102-111.
23. K. F. Liu, S. J. Xie, H. J. Wei, X. J. Li, S. L. Liu, L. Y. Xu. Appl. Catal. A: Gen., 2013, **468,** 288-295.

24. B. Zhang, Y. J. Ji, Z. D. Wang, Y. M. Liu, H. M. Sun, W. M. Yang and P. Wu. *Appl. Catal. A: Gen.,* **443-444 ,** 103-110

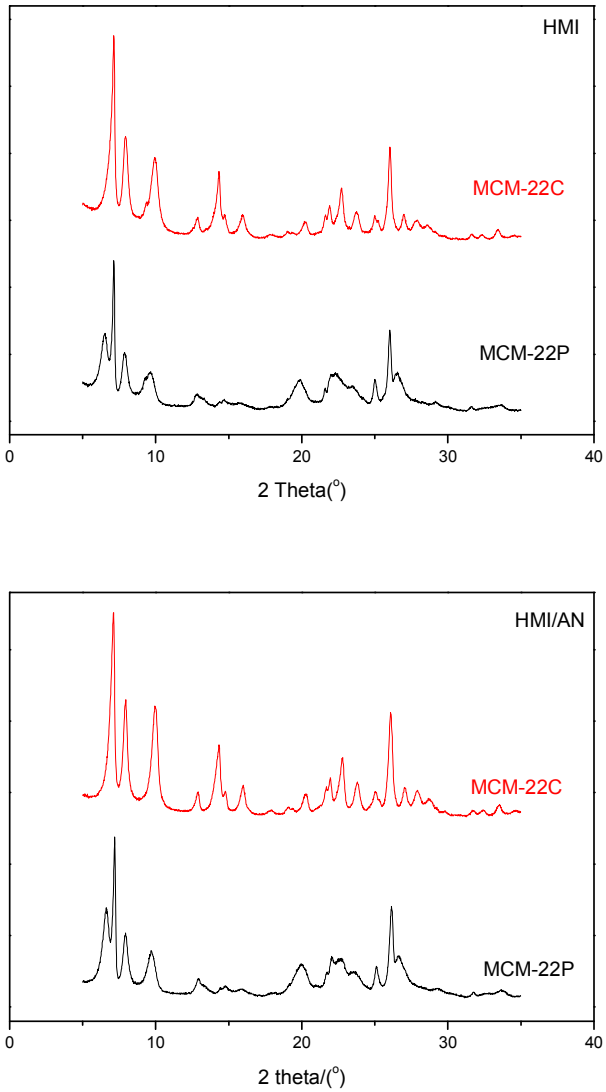

Fig. 1 XRD patterns of MCM-22 zeolites (SiO_2/Al_2O_3 = 30)

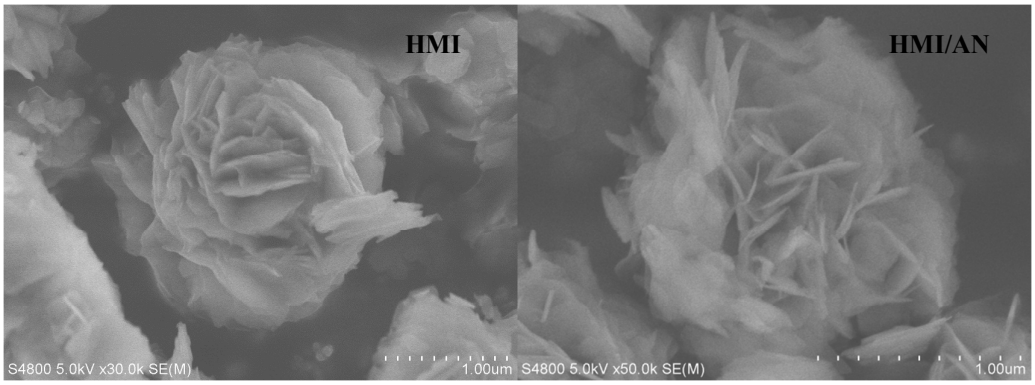

Fig. 2 SEM images of MCM-22C zeolites

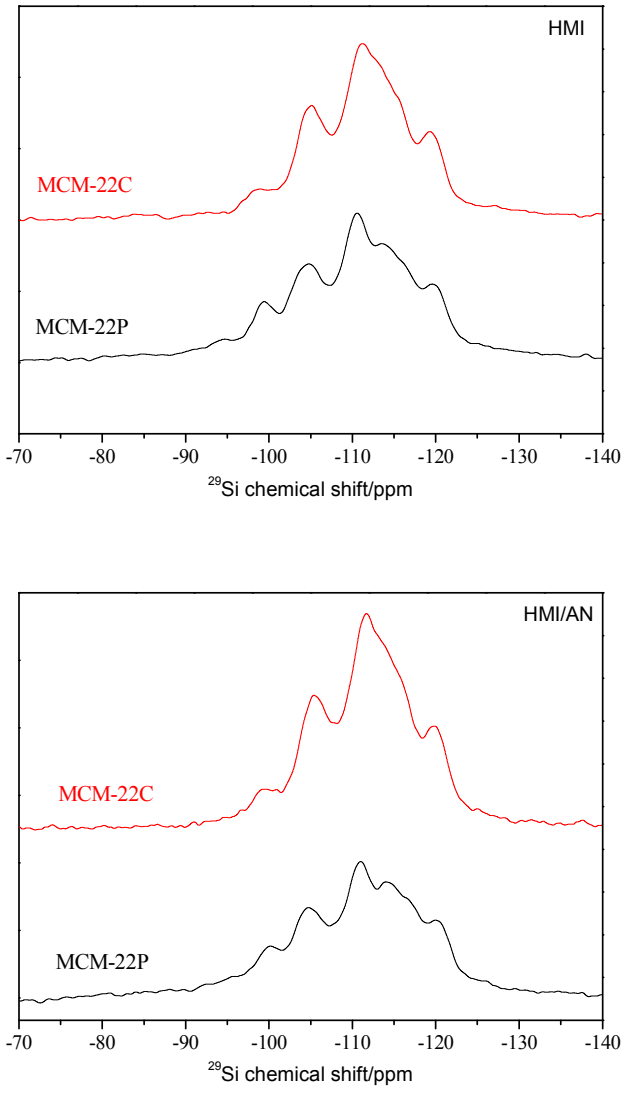

Fig. 3 ^{29}Si MAS NMR spectra of MCM-22 zeolites (SiO_2/Al_2O_3 = 30)

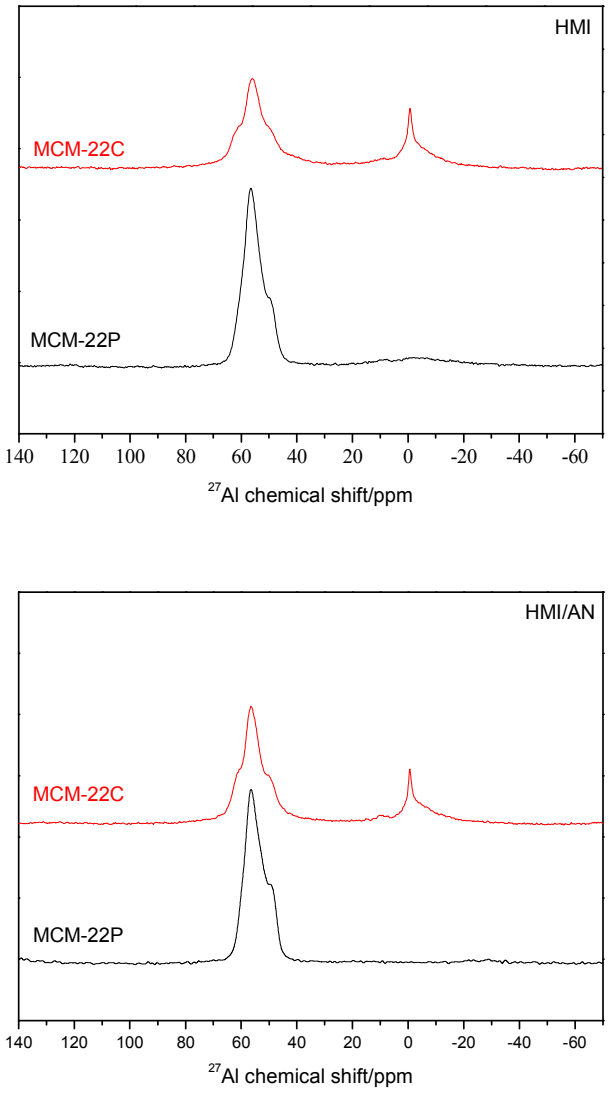

Fig. 4 ^{27}Al MAS NMR spectra of MCM-22 zeolites (SiO_2/Al_2O_3 = 30)

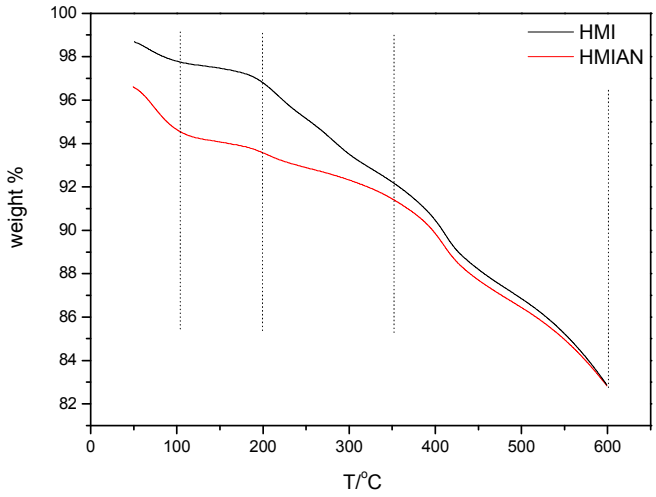

Fig. 5 TG curves of MCM-22P zeolites (SiO_2/Al_2O_3 = 30)

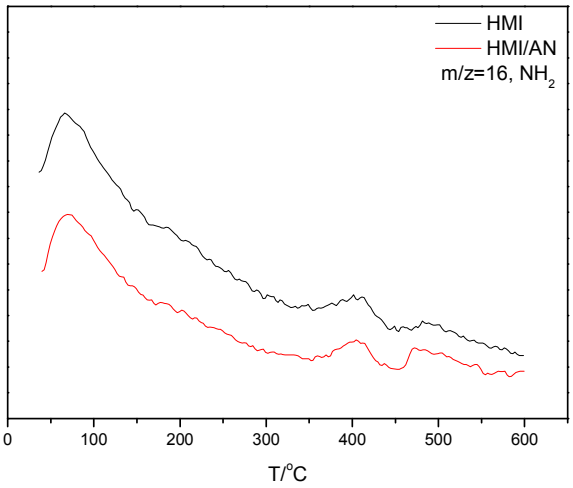

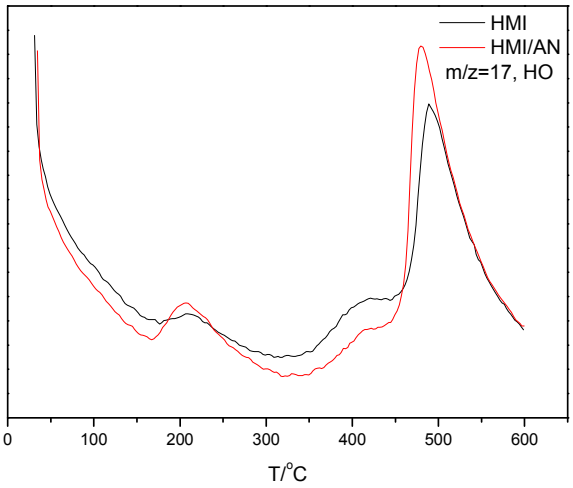

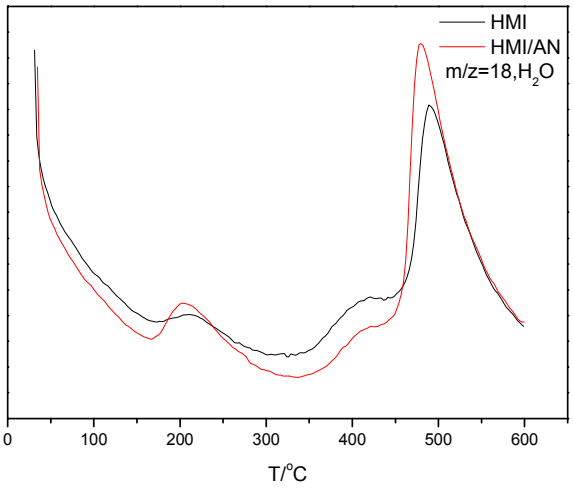

Fig. 6 TG-MS curves of MCM-22P zeolites (m/z = 16, 17 and 18)

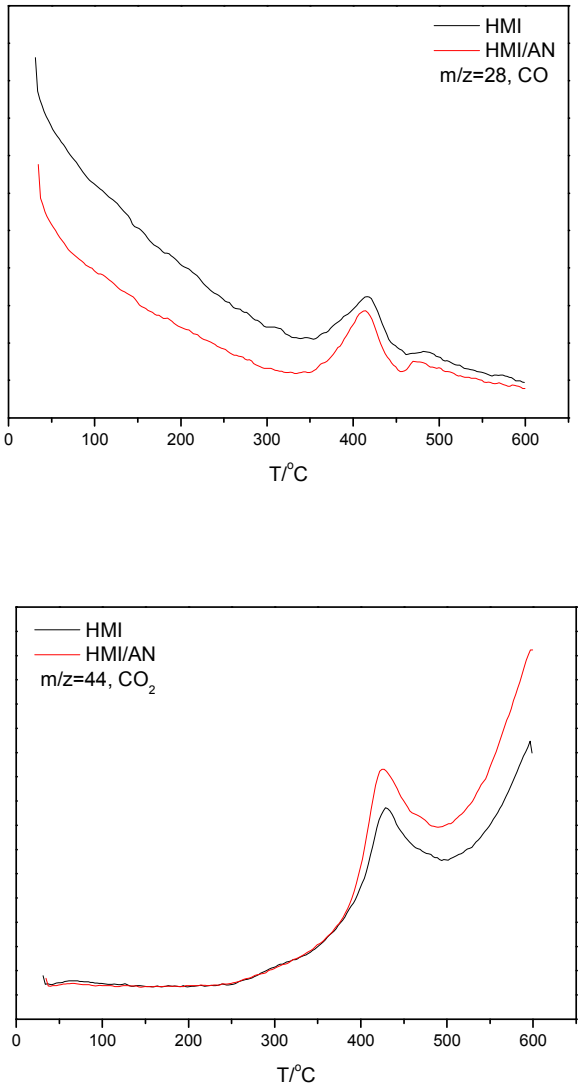

Fig. 7 TG-MS curves of MCM-22P zeolites (m/z = 28 and 44)

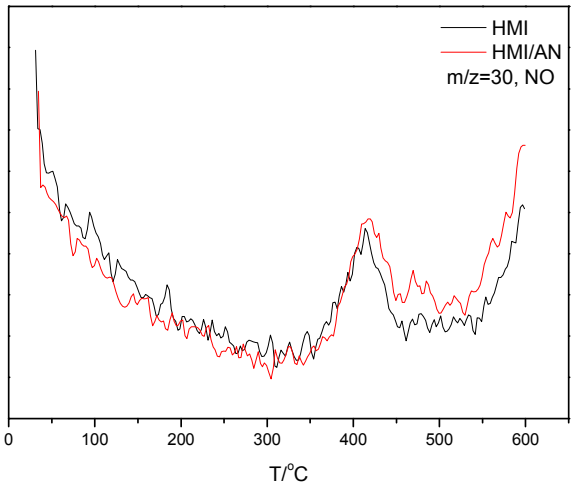

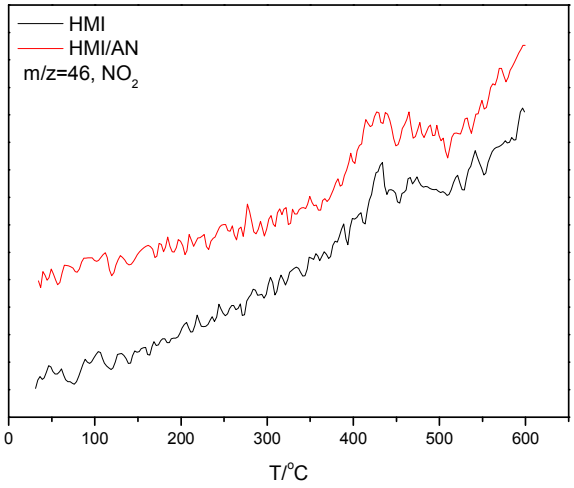

Fig. 8 TG-MS curves of MCM-22P zeolites (m/z = 30 and 46)

Table 1 Hydrothermal synthesis of MWW zeolites in HMI and HMI/AN systems

Template	SiO_2/Al_2O_3		HMI/SiO_2	AN/SiO_2	Phase
	gel	product			
HMI	30	26.2	0.30	0	MCM-22
HMI	25	22.7	0.30	0	MCM-22
HMI	20	18.7	0.30	0	MCM-49
HMI/AN	30	26.4	0.10	0.20	MCM-22
HMI/AN	25	22.8	0.10	0.20	MCM-22/49(more)
HMI/AN	20	18.6	0.10	0.20	MCM-49

Table 2 Textural properties of MCM-22C zeolite (SiO_2/Al_2O_3=30.0)

Samples	SiO_2/Al_2O_3		S_{BET}/m^2·g^{-1}	S_{micro}/m^2·g^{-1}	V_{total}/cm^3·g^{-1}	V_{micro}/cm^3·g^{-1}
	gel	product				
HMI	30.0	26.2	469	379	0.592	0.173
HMI/AN	30.0	26.4	462	382	0.534	0.178

Table 3 Alkylation of benzene with ethylene over H-MCM-22 (HMI) and H-MCM-22 (HMI/AN) catalysts

	T/°C	200	210	220	230	240	250	260
HMI catalyst	Ethylene conversion %	97.5	97.7	97.9	98.6	99.4	99.8	99.9
	EB selectivity %	89.2	86.8	85.5	85.0	84.6	84.2	84.0
HMI/AN catalyst	Ethylene conversion %	97.4	97.9	98.0	98.7	99.7	99.9	99.9
	EB selectivity %	89.2	84.5	85.1	84.2	83.5	83.1	82.4

Table 4 The distributions of DEBs and TEBs at 200 °C

Wt. %	m-DEB	p-DEB	o-DEB	∑DEB	1,3,5-TEB	1,2,4-TEB	1,2,3-TEB	∑TEB
HMI	1.25	1.12	1.86	4.23	0.009	0.124	0.043	0.176
HMI/AN	1.19	1.07	1.77	4.21	0.007	0.126	0.051	0.184